International Journal of Technology 15(4) 999-1011 (2024)
Received June 2022 / Revised December 2022 / Accepted September 2023

International Journal of Technology

http://ijtech.eng.ui.ac.id

Adhesives Type on the Burning Rate and Emission Properties of Honeycomb Sandwich Composite

I Gusti Agung Ketut Catur Adhi[1], Ketut Adi Atmika[2,4], Ni Made Dwidiani[2], I Dewa Gede Ary Subagia[2,3,4*]

[1]*Department of Mechanical Engineering, Mataram University, Nusa Tenggara Barat, 83121, Indonesia*
[2]*Mechanical Engineering Study Program, Udayana University, Bukit Jimbaran 80361, Badung-Bali, Indonesia*
[3]*Materials Engineering Laboratory, Engineering Faculty, Udayana University, Bukit Jimbaran 80361, Badung-Bali, Indonesia*
[4]*Technology and Material Research Centre, the Institution of Research and Community Service, Udayana University, Bukit Jimbaran 80361, Badung-Bali, Indonesia*

Abstract. Sandwich composite is an important part of engineering products capable of replacing metallic composite. It consists of two types of material, namely polypropylene honeycomb core and skin made from jute fiber-reinforced epoxy composite (JFRP), which are joined with glue. This study presented a unique discussion about adhesives that focused on the burning rate and emission performance of S_{A-A} and SD-E. The burning rate performance was assessed with the UL-94 HB test in accordance with the ASTM D 635 standard. Emission value of both adhesives was also examined in line with the ASTM D 2863 standard using a Gasboard-3100P Syngas analyzer. In addition, FTIR and SEM analyses were used to determine the characteristics of the S_{A-A} and S_{D-E} adhesives. The results showed a significant difference in adhesives rates, with S_{A-A} burning 0.5% faster than S_{D-E} in addition to a 0.58% reduced weight loss. Emission test confirmed that both adhesives have similar LOI values of 22.6% and 22.8%, respectively. S_{A-A} adhesives contained LSD, which is dangerous to human health. In conclusion, S_{D-E} adhesives should be used on sandwich composite due to its epoxy-based potential as a flame retardant because S_{A-A} adhesives has more potential to trigger firing due to the fuel content.

Keywords: Adhesives; Burning rate; Emission; Fire; Sandwich composite

1. Introduction

Sandwich composite structures are widely used in manufacturing engineering products, and it consist of three components, namely skin, core and adhesives (Jeevi, Nayak, and Abdul-Kader, 2019; Novotný, Doubrava, and Růžička, 2017). The thick core is covered by a pair of thin skins (Wei *et al.*, 2020). Sandwich composite structures are characterized by the lightweight nature, production ease, strong mechanical properties and are highly used in manufacturing airplanes, automobiles, ships, and packaging, including electrical insulators, energy absorption, and other industrial purposes (Rupani, Acharya, and Jani, 2017).

Failure caused by fire has become increasingly relevant in recent years (Suwondo *et al.*, 2021), despite the numerous benefits of composite materials, one significant disadvantage

*Corresponding author's email: arsubmt@unud.ac.id, Tel.: +62 81353651467
doi: 10.14716/ijtech.v15i4.5728

is the highly inflammable nature (Zhu *et al.*, 2020). Fire performance was determined based on factors such as ignition, self-extinguishing ability, flame spread, burn through, heat release, smoke obscuration, toxicity, and related scenarios. Therefore, the process of assessing the resistance of composite materials is needed to examine the ability to perform the intended load-bearing functions when exposed to fire. Several studies have extensively examined fire performance of composite materials (Ortega *et al.*, 2020; Hörold *et al.*, 2017; Suoware, Ezema, and Edelugo, 2017; Salmeia *et al.* 2016; Bar, Alagirusamy, and Das, 2015; Szolnoki *et al.*, 2015). However, the most widely accepted study focused on an experiment conducted by incorporating fire retardant into the polymer matrix. The aim was to suppress heat release, increased temperature, and gas emission, perceived as toxic sources, through the solid and gaseous phase mechanism (Ogabi *et al.*, 2021; Kim, Dutta, and Bhattacharyya, 2018).

These properties need to be considered when studying the combustibility of honeycomb-based composite materials. According to Kim, Dutta, and Bhattacharyya (2018), several factors such as the chemical composition, physical features, load-bearing capacity of adhesives, surface condition of the joints, and the use of materials that do not adhere to health standards significantly affect the toxicity of emitted smoke (Jeevi, Nayak, and Abdul-Kader, 2019; Ledesma *et al.*, 2018). Preliminary studies stated that synthetic adhesives, such as structural silicone, or stiffer substances namely acrylic or epoxy are commonly used for assembling composite materials (Shang *et al.*, 2020; Valente *et al.*, 2019; Ledesma *et al.*, 2018; Machalická and Eliášová, 2017). However, thermosetting types such as phenol-formaldehyde (PF), urea-formaldehyde (UF), and polyurethane (PU) are currently been used due to the water-resistant properties (Chanda, Kim, and Bhattacharyya, 2022; Shavandi and Ali, 2018). The application of adhesives in non-metallic structural materials has numerous benefits, including uniform stress distribution, eliminating the need for drilling, and enabling the bonding of substances with varying mechanical and thermal properties. Sugiman and Sulardjaka (2016), stated that adhesives play a critical role in the bonding of materials. Arenas, Narbón, and Alía (2010), stated that joint strength is inversely proportional to the thickness of adhesives, meaning the shear strength increases as the thickness of adhesives decreases. Davies *et al.* (2009), examined the physical, chemical, and mechanical properties of Aluminium substrates bonded with epoxy adhesives of varying thicknesses ranging from 0.2 to 1.3 mm. However, there is no proof that varying thickness can weaken composite materials (Kostin, Nasonov, and Zinin, 2021; Momber, Fröck, and Marquardt, 2021; Shang *et al.* 2020; Jeevi, Nayak, and Abdul-Kader, 2019; Shavandi and Ali, 2018).

Adhesives are an essential aspect of sandwich composite structures that bond the core and skin. Generally, the liquid types such as $S_{A\text{-}A}$ and $S_{D\text{-}E}$ are commonly used due to ease of application. Aica-Aibon ($S_{A\text{-}A}$), a kind of poly-chloroprene-based glue with toluene characteristics (C_7H_8) (Tualeka *et al.*, 2019; Djurendić-Brenesel, Stojiljkovic, and Pilija, 2016), contains lysergic acid diethylamide (LSD) with the chemical formula $C_{20}H_{25}N_3O$. LSD is a synthetic narcotic drug that causes mental disorders when consumed excessively. Liao *et al.* (2020) stated that when $S_{A\text{-}A}$ is burned, it tends to have minimal impact on the surrounding environment. Meanwhile, Dextone-Epoxy ($S_{D\text{-}E}$) is an epoxy-based adhesive dependent on epoxy resin and one of the most essential polymer classes due to the multiple binding capacities provided by the oxirane ring. Due to the significant differences in the source materials, studying the flame and emission of these adhesives becomes interesting. This study mainly focused on examining the impact of flammability and emission on adhesives used in sandwich composite. Furthermore, both adhesives were tested concerning the application process in honeycomb composite to evaluate burning rate and emission. The aim is to investigate the potential roles as triggers for fuel fire and the resulting emission. The tests were carried out based on ASTM D 635 and 2863 standards to determine both adhesives burning rate and emission.

2. Materials and Methods

2.1. Materials

Sandwich composite panel comprised three main parts, namely skins, adhesives, and honeycomb core. A typical example is the natural jute fiber, produced by Casthanal Textile CIA in Brazil, shown in Figure 1 (Gupta, Srivastava, and Bisaria, 2015). The fiber has relatively low conductivity, ranging from 0.29 to 0.32/mK, as well as composite matrix materials, namely Bakelite Korea epoxy resin Bakelite-EPR-174 and Justus Kimia-Raya cycloaliphatic amine curing agent Bakelite-EPH-555, shown in Tables 1 and 2.

Polypropylene honeycomb (PPH), particularly a Nomex 8 mm mesh, was used as the core of composite sandwich. This material has a low density and good performance function as a shear load-carrying core in sandwich composite construction. PPH is a hexagonal structure with equal sides and six interior angles of the same dimension measuring 120^0, as shown in Figure 2.

The study used adhesives $S_{A\text{-}A}$ and $S_{D\text{-}E}$ supplied by PT AICA- Indonesia and PT Dextone Lemindo, Japan, respectively. $S_{A\text{-}A}$, composed of 10 to 99 wt.% ethylene-vinyl acetate copolymer adhesives, is produced by dissolving rubber in liquid solution, thereby producing a yellow colour. Although $S_{A\text{-}A}$ showed outstanding substrate adhesion characteristics of the toluene (C_7H_8) class, it contained an LSD compound hazardous to human health. The specific properties of these adhesives are shown in Table 3.

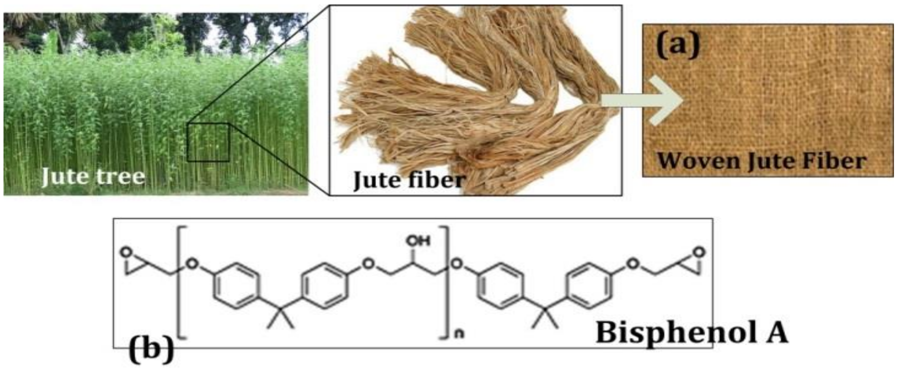

Figure 1 a) Seedbed process of jute fiber, b) chemical bonding of epoxy bisphenol A

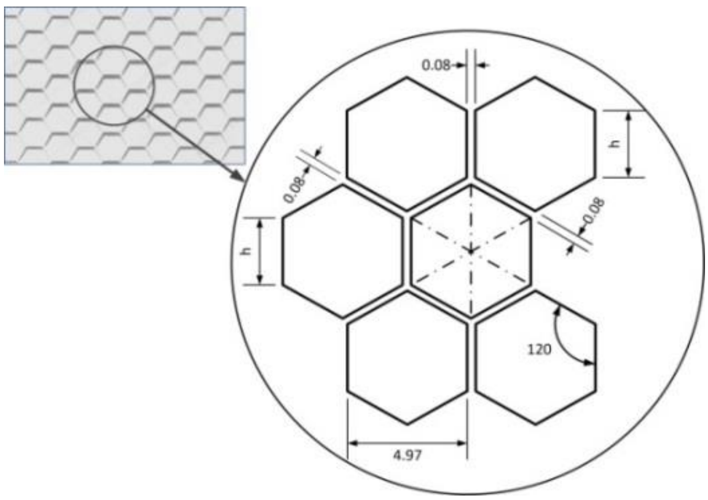

Figure 2 Geometry and cross-section of honeycomb

After S_{D-E} is an epoxy-based adhesive containing epichlorohydrin bisphenol-A (DGEBA) in the formulation. Epoxy resin is characterized by low-molecular-weight comprised of oxirane or epoxide rings as functional groups, imparting thermosetting properties. This makes epoxy resin a commonly and widely used material in various applications, including adhesives, coatings, semiconductor packaging, and composite matrices. The specific S_{D-E} adhesive characteristics are shown in both Tables 2 and 3.

Table 1 Mechanical and physical properties of jute fibre as reinforcement in the shell of sandwich composite

Properties	Jute fibre
Cellulose (wt.%)	61–72
Lignin (wt.%)	12–13
Hemicellulose (wt.%)	13.6–20.4
Ash (%)	0.5–2
Micro fibrillary (%)	8.0
Density (g/cm^3)	1.46
Tensile strength (MN/m^2)	400–800
Young's modulus (GPa)	10–30
Specific modulus	7–21
Elongation to break (%)	1.8
Moisture absorption (%)	12

Table 2 Properties of epoxy and hardener

Properties	Epoxy	Hardener
Density (g/cm^3) 25^{o}C	$1.17^{\pm 0.02}$	1.01
Tension strength (MPa)	58.8	55.15
Modulus Young's (GPa)	5.0	3.0
elongation (mm/mm)	4	6
Viscosity (mPa-s) (poise)	$0.13^{\pm 0.02}$	0.5~1.0

Table 3 Properties of Synthetic adhesives

Properties	Aica-Aibon	Dextone Epoxy
Physical state	Liquid, Toluene	Viscous liquid
Density (g/ml)	N/A	1.10
Tensile strength (Psi)	-	7526
Heat resistance (C)	-	120
Hardness	Low	90-92
Viscosity 20^{o}C (cps)	$3500^{\pm 300}$	3500
Specific Gravity	1.6	1.6
Drying time (h)	2.4	3
bonding force kg/cm^2	$10\text{-}13^{\pm 2}$	>13
Flash point F (C)	39.2 (4.0)	230 (204)
Combustion products	CO_2	CO_2, Aldehydes, Acid Vapors
Toxicological	Skin, Eyes irritation	skin irritation
Boiling Point/Range (C)	110 ~ 111	>200
Hazard	aromatic	aromatic
Flammability limits (%)	N/A	N/A

2.2. Sandwich composite structures

Sandwich composite panel used in the experiment was 350 mm x 350 mm in size. A panel with three layers of 2 mm thick jute fiber reinforcement was used as the skin of composite. In addition, the panel was manufactured using the vacuum injection process (VaRTM), with the core bonded to both skins using two different types of synthetic adhesives. Figure 3 and Table 4 show sandwich composite and specimen structures using both S_{A-A} and S_{D-E} adhesives, respectively.

Figure 4 shows the geometry of the sample and burning test schema following the ASTM D 635 standards. The specimen used was composed of three segments measuring 125 mm in length. The first segment, positioned 25 mm from the free end, was the initial burning area. The subsequent and final ones, which served as burning test and clamping areas, were 75 mm and 25 mm long, respectively.

Table 4 Sandwich composite materials

Samples	Skin	Core	Adhesive
$S_{(A-A)}$	JFRP	PP-Honeycomb	Aica-Aibon
$S_{(D-E)}$	JFRP	PP-Honeycomb	Epoxy Dextone

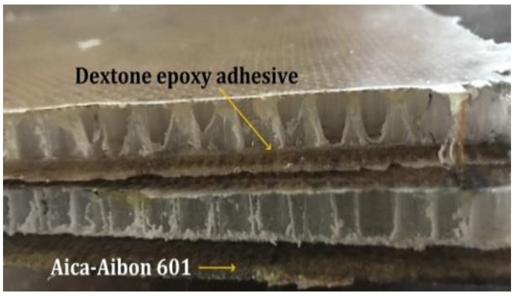

Figure 3 Bottom-part sandwich composite panels with S_{A-A} adhesives and top-part sandwich composite panels with S_{D-E} adhesive

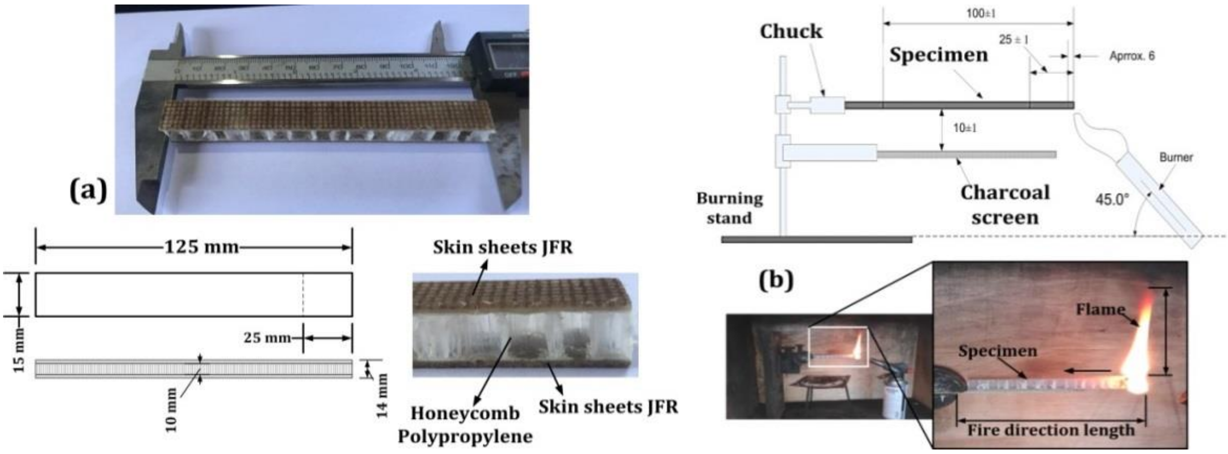

Figure 4 a) Size and design of sandwich composite with SAA and SDE adhesives, b) The burn test process of the samples carried out with UL-94HB in the combustion chamber

2.3. Analytical Method

The burning resistance of the sample was tested under the UL-94HB (Chukwunwike *et al.* 2019) and LOI value (Lee, Salit, and Hassan, 2014) following the ASTMD 2863 standards. UL-94HB is a standard for evaluating the flammability safety of plastic materials used as parts of devices. The test was conducted through slow burning in a horizontal position of the specimen, shown by the HB code. In addition, emission gas was tested using a Syngas analyzer gas bord-3100P. The LOI value was determined following equation 1 (Szolnoki *et al.*, 2015):

$$LOI = 100 \times \frac{[O_2]}{([O_2]+[N_2])} \tag{1}$$

Sandwich composite burning propagation was determined using equation 2 as follows:

$$FP = \frac{D_p}{(P_t - L_t)} \tag{2}$$

Burning rate (Misnon *et al.*, 2018) was determined using equation 3:

$$V = \frac{(L \times 60)}{t} \tag{3}$$

where LOI is the limiting oxygen index (%) (Parmar *et al.* 2014), O_2 and N_2 are denoted as oxygen and nitrogen. L is the distance between two marking lines (75 mm), t is fire spreading time (minutes), FP is the flame propagation (mm/second), D_p is the propagation distance (mm), P_t is fire propagation time (second), and L_t is burning time (second).

The weight loss of the specimen was determined using equations 4 and 5:

$$w = w_0 - w_1 \tag{4}$$

$$W = \frac{w}{t} \tag{5}$$

where W is the total weight loss after burning (gram/sec), w is the weight loss of the specimen during the burning process, w_0 is the initial weight (gram), w_1 is the final weight (gram), and t is the burning time (second).

2.4. FT-IR spectroscopic analysis

The characteristics of adhesives in sandwich composite were measured using Fourier transform infrared spectroscopy (FTIR) spectra obtained with a Shimadzu spectrometer. The signal resolution of the FTIR was 1 cm^{-1}, and a minimum of 16 scans were obtained and averaged within the range of 500 to 4000 cm^{-1}.

2.5. Scanning electron microscopy (SEM)

The residue from the horizontal burning test on sandwich composite was subjected to SEM analysis using a JSM-6510 from Japan. In addition, the residue surface was coated with gold before being tested.

3. Results and Discussion

3.1. FTIR analysis

Figure 5 shows the FTIR spectra of the $S_{A\text{-}A}$ and $S_{D\text{-}E}$ adhesives used to bond the skin to the core of the sandwich composite. The test results show different performances for each adhesive, with $S_{A\text{-}A}$ and $S_{D\text{-}E}$ adhesives being rubber-based and monomers from the diglycidylether bisphenol A (DGEBA) family, respectively.

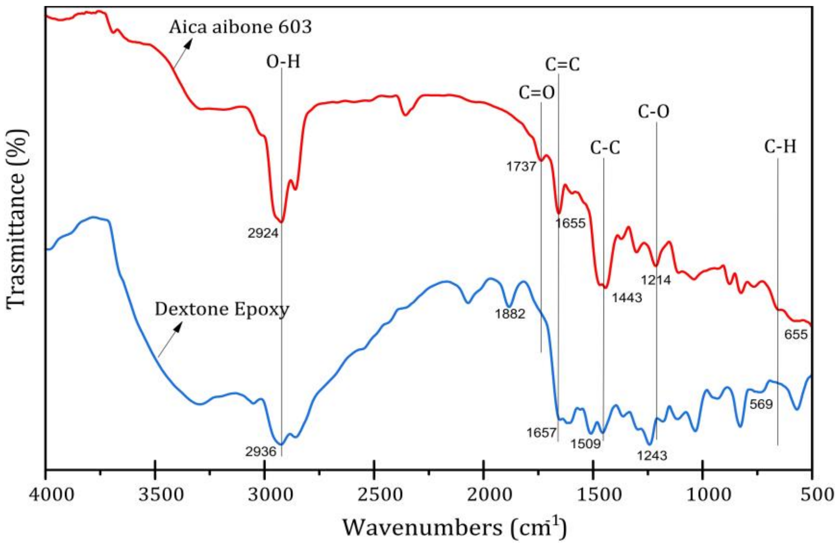

Figure 5 FT-IR spectra pattern adhesives of $S_{A\text{-}A}$ and $S_{D\text{-}E}$

Analysis of the FTIR spectra comparing the S_{A-A} (red line) and S_{D-E} adhesives (blue line) shows significant differences. The O-H stretching region in the absorbance range of 2500 cm^{-1} to 3000 cm^{-1} showed there was a peak shift of 2936 cm^{-1} and 2924 cm^{-1} for S_{D-E} and S_{A-A}. However, within an absorbance range of 2000 cm^{-1} to 2500 cm^{-1}, S_{D-E} had increased energy compared to S_{A-A}, depicting a greater tendency for bond breaking, thereby contributing to enhanced stability and reduced flammability. The characteristic peaks for C-O-C ether and aromatic C-C stretching were observed at 1036 cm^{-1} and 1509 cm^{-1}, respectively. The stretching C=C in the aromatic ring was observed at 1608 cm^{-1}, while C-H bending bands occurred within the absorbance range of 500 cm^{-1} to 1000 cm^{-1}.

3.1. *Burning Rate*

The recent focus on building fire has proven the importance of understanding the material types used (Suwondo *et al.,* 2021). Building materials and equipment types have been identified as the main factors contributing to the frequency of these fire (Nugroho, Latief, and Wibowo, 2022). The combustibility of a material depends on various factors related to the constituents, which impact characteristics such as heat release, flame spread, and ignitability (Pausas, Keeley, and Schwilk, 2017). In addition, the presence of adhesives used to bond the skin and core of sandwich composite was considered fire reaction properties, as shown in Table 5.

Table 5 Characteristics of combustion products and weight loss of sandwich composite with SDA and SDE adhesives on sandwich composite

Adhesive type	Code	Burning Length (mm)	Burning Time (minutes)	Burning rate V (mm/min)	Weight losses W (gr/min)
Aica-Aibon	S_{A-A}	75	2.15	$34.91^{\pm1.38}$	$3.17^{\pm0.41}$
Dextone epoxy	S_{D-E}	72	4.14	$17.40^{\pm1.38}$	$1.32^{\pm0.41}$

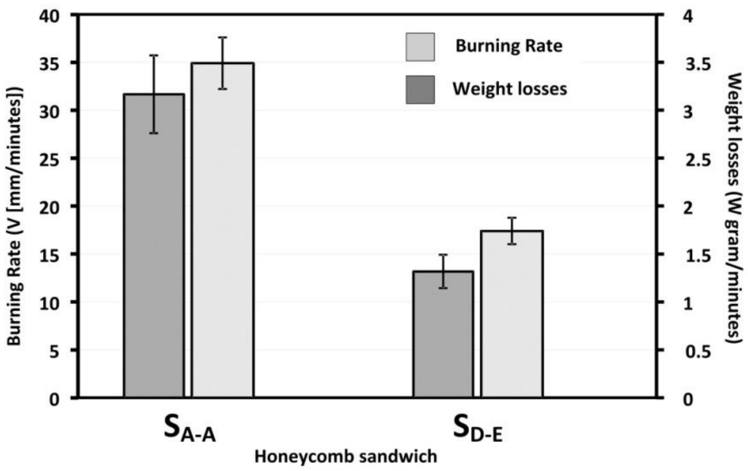

Figure 6 Comparison of adhesives on burn test and weight loss of honeycomb composite

Figure 6 shows a bar graph of burning rate and weight-loss combination of sandwich composite using S_{A-A} and S_{D-E} adhesives. The use of dark colour shows there is a significant difference in burning rate between sandwich composite using S_{A-A} and S_{D-E}. This was caused by the different chemical compound properties of both adhesives, as shown in Figure 5. S_{A-A} is an elastomer-based adhesive that can function as thermoplastic and thermosetting types, depending on the required cross-linked structure. It is also characterized by rapid adhesion and belongs to a group of elastomers with rubber-based adhesives, including butyl, butadiene, styrene-butadiene, and nitrile rubber, as well as silicone, and neoprene

(Wang *et al.*, 2022). However, adhesiveness and cohesion levels are limited at temperatures greater than 70°C, and a stabilizer is needed to withstand environmental effects such as UV and ozone. Adhesives can be dried at normal temperatures and has good heat, water, and chemical resistance, depending on the contents of the hardening compounds. S_{A-A} adhesives characterized based on FTIR analysis, showed features of a rubber-based composition, for example, C=C aromatic bonds observed at a wavenumber of 1656.92 cm^{-1}. Meanwhile, the aliphatic C-H or C-C hydrocarbon groups that trigger the flame were observed in the wavenumber range of 2000 cm^{-1} to 2500 cm^{-1} with a prominent peak at 2358.08 cm^{-1} and an intensity of 79.64 µm. S_{D-E} adhesives are epoxy-based, mainly synthesized from active hydrogen reactions in phenols, alcohols, amines, and acids with epichlorohydrin under well-controlled conditions. Generally, S_{D-E} adhesives were prepared by packing epoxy and curing agent composition separately before use, with curing occurring briefly after mixing in accordance with the mixing ratio. Epoxy adhesives such as S_{D-E} often have a higher glass transition temperature, making it suitable for applications requiring high-temperature resistance. In FTIR analysis, the epoxy tends to react with amines and amides (NH) at frequencies ranging from 3140 to 3320 cm^{-1}. The deformation band of C-O occurred at 828.46 cm-1 within the wavenumber range of 750 cm^{-1} to 1000 cm^{-1}. In the spectrum range, characteristics of the aromatic ring were observed, double chain, benzene and C-C aromatics, C-O-C chain from the ether, C-O chain of oxirane group, and CH_2 chain were formed at wavenumbers of 1606 cm^{-1}, 1506 cm^{-1}, 1031 cm^{-1}, 913 cm^{-1}, 862 cm^{-1} and 769 cm,$^{-1}$ respectively. The stretching of hydroxyl groups of O-H was depicted by broadband at 3500 cm^{-1}, suggesting the presence of species and dimers of high molecular weight. In addition, a band corresponding to the ether linkage was observed within the 1000 to 1100 cm^{-1} spectrum range.

The average combustion length of the S_{A-A} and S_{D-E} adhesives was 75 mm and 72 mm, respectively. The results showed the carbon composition of the S_{A-A} adhesives possessed higher fuel propagation capacity compared to the S_{D-E}, which had greater fire resistance. This result is in line with the study conducted by Chanda, Kim, and Bhattacharyya (2022), focusing on the significant influence of adhesive formulation materials on fuel value. The burning rate of each sandwich composite sample using the S_{A-A} adhesives was 0.5% faster than the S_{D-E}. The difference was caused by certain thermos-physical properties, such as the reaction rate depending on the temperature threshold or higher amount of oxygen (O_2) during the combustion process, leading to increased heat energy (Ogabi *et al.,* 2021). Table 5 shows the burning time of the two adhesives used.

In Figure 6, the result of the weight loss measures in the bar graph is shown in grey. The result is similar to the burning rate, and the weight loss of S_{A-A} adhesive samples has a higher value than $S_{D-E,}$ with a significant difference of 0.58%. This difference directly correlates with the degradation of the samples caused by increased heat and smoke production. The higher weight loss and low percentages of mass residues observed in the S_{A-A} samples were attributed to the pyrolysis and burning phases, depicting a prolonged exposure to heat flux. These results are in line with previous studies (Vinod *et al.*, 2022).

Table 6 The average values of chemical elements of S_{A-A} and S_{D-E} adhesives

Adhesive type	Code	CO (mg/m^3)	CO2 (mg/m^3)	CxHx (mg/m^3)	HC2 (mg/m^3)	O2 (mg/m^3)	NO2 (mg/m^3)	LHV (MJ/m^3)
Aica-Aibon 601	S_{A-A}	0.358	6.92	0.01	0.088	20.964	71.658	0.01
Dextone Epoxy	S_{D-E}	0.548	7.7	0.004	0.128	20.942	70.7	0.018

3.2. Burning Emission

Table 6 shows emission from burning sandwich composite, which were tested to determine the environmental effects of burning adhesives. When burned, adhesives in composite emits carbon dioxide (CO_2) and carbon monoxide (CO) as combustion products, which is proven by the results of the FTIR test shown in Figure 5. However, both S_{A-A} and S_{D-E} adhesives generated the same quantity of oxygen, measured at 20.9 mg/m^3. The NO_2 produced by the S_{A-A} adhesives is slightly greater than S_{D-E} by 0.01%, the two materials have similar LOI values of approximately 22.6% and 22.8%, respectively. The difference in burning behavior was caused by the higher carbon content in S_{D-E}, which formed a denser carbon layer, preventing heat transfer during the burning process. There is a definite relationship between burning rate and oxygen content, with a threshold of 21%. Materials with an LOI less than this threshold are typically regarded as flammable or combustible and would burn readily in an open-air setting, while a higher index showed lower flammability (Raajeshkrishna and Chandramohan, 2020). When the oxygen content drops below the critical LOI values, the material ceases to burn because the available oxygen is insufficient for combustion. However, a high LOI value, minimizes burning potential and oxygen concentration, in order to sustain combustion (Misnon *et al.*, 2018). LOI is a distinguishing characteristic of materials, often used to rank the relative flammability of polymer composite materials (Raajeshkrishna and Chandramohan, 2020; Chukwunwike *et al.*, 2019; Bhattacharyya and Kim, 2017).

3.3. Burning residue

Figures 7a and b show the charcoal from sandwich composite with S_{A-A} and S_{D-E} adhesives, respectively. The characteristics of the charcoals depend on the quantity of lignin and cellulose content in the jute fiber and properties of the polypropylene in the core. Furthermore, Charcoal produced from poly-propylene is more reflective and contains the following compounds CO, CO_2, HC_2, NO_2, and C_xH_x. The elements produced from combustion are also described in the spectral range of the FTIR test for each adhesive applied in the bonding of sandwich composite. This implied that the chemical breakdown of each adhesive sample contributed to the formation of oxides and other degradation products, forming the crosslinking network that produced the coal. Meanwhile, the LSD element contained in the S_{A-A} adhesives was in the form of C_xH_x, which is harmful when inhaled.

Figure 8 shows the result of the SEM test conducted on the charcoal samples obtained after burning, showing distinctive structural characteristics. The charcoal samples from S_{A-A} and S_{D-E} adhesives had rubber and polymer-based structures that are not agglomerated, respectively, as shown in Figures 8a and b.

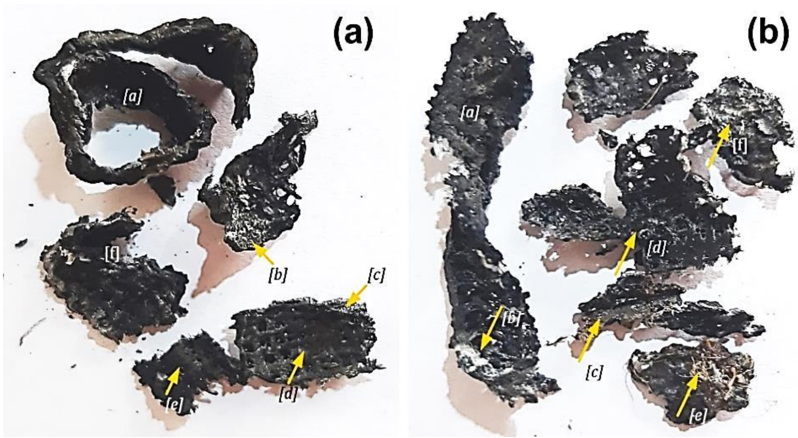

Figure 7 a) S_{D-E} adhesive residue for sandwich honeycomb composite**;** b) S_{A-A} adhesive residue type of sandwich composite during the burning

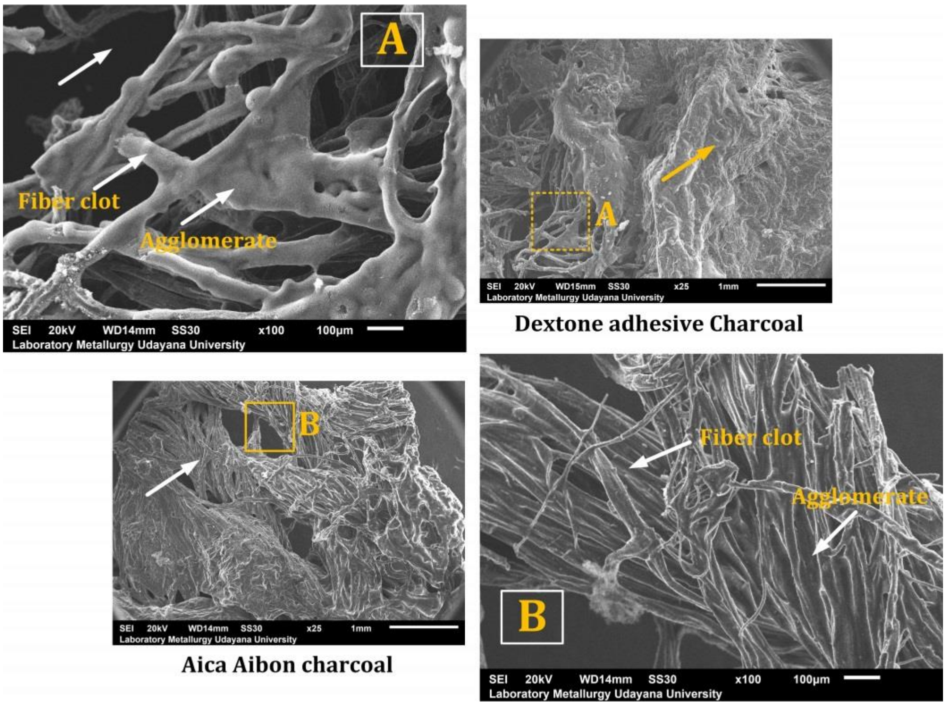

Figure 8 Photography SEM adhesive residue after the burning process. a) SEM S_{D-E} adhesives, b) SEM S_{A-A} adhesives

4. Conclusions

In conclusion, adhesives were critical in sandwich composite structures, directly impacting the burning rate. To address the flammability of composite, it was necessary to incorporate materials or substances capable of inhibiting the burning rate. Synthetic adhesives such as S_{A-A} and S_{D-E} were used to bond the skin to the core of sandwich composite. The results showed that sandwich composite's burning rate using S_{A-A} adhesives was 0.5% faster, with a weight loss of 0.58% greater than S_{D-E}. Emission test results for both samples had a comparatively similar LOI value of 22.6% and 22.8%, respectively. Therefore, adhesives significantly impacted burning rate and composite emission, depending on the presence of flammable substances contained in the constituents. The S_{A-A} adhesives posed a significant risk when burned due to its aromatic nature and the presence of LSD elements, which could be harmful when inhaled. However, S_{D-E} adhesives only showed the aromatic properties when burned. The use of S_{A-A} adhesives on sandwich composite materials posed a greater risk compared to S_{D-E}. This was due to the potential of S_{A-A} adhesives to ignite more intense fire attributed to the contained benzene. So, it was suggested that using S_{A-A} adhesives in materials subjected to high temperatures and susceptible to flammability be avoided.

Acknowledgments

The authors are grateful to the Institution of Research and Community Service for their financial support. The authors are also grateful to the Udayana University and the Indonesian Ministry of Education, Culture, and Research for the grant under contract number B/136-8/UN14.4.A/PT.01.05/2021.

References

Arenas, J.M., Narbón, J.J., Alía, C., 2010. Optimum Adhesive Thickness in Structural Adhesive

Joints Using Statistical Techniques Based on Weibull Distribution. *International Journal of Adhesion and Adhesives*, Volume 30(3), pp. 160–165.

Bar, M., Alagirusamy, R., Das, A., 2015. Flame Retardant Polymer Composites. *Fibers and Polymers*, Volume 16(4), pp. 705–717

Bhattacharyya, D., Kim, N.K., 2017. Flammability of Natural Fiber-Reinforced Polymeric Composites. *In:* ICCM International Conferences on Composite Materials, Volume 2017, pp. 1–9

Chanda, A., Kim, N.K., Bhattacharyya, D., 2022. Effects of Adhesive Systems On The Mechanical and Fire-Reaction Properties of Wood Veneer Laminates. *Composites Science and Technology*, Volume 230, p. 109331

Chukwunwike, S.A., Ike-Eze, I.E., Aigbodion, V.S., Okafor, K.J., 2019. Flammability Properties of Flame Retarded Natural Fiber Reinforced Polymer Composites: An Overview. *Journal of Materials and Environmental Sciences,* Volume 10(7), pp. 647–656

Davies, P., Sohier, L., Cognard, J.Y., Bourmaud, A., Choqueuse, D., Rinnert, E., Créac'hcadec, R., 2009. Influence of Adhesive Bond Line Thickness on Joint Strength. *International Journal of Adhesion and Adhesives*, Volume 29(7), pp. 724–736

Djurendic-Brenesel, M., Stojiljkovic, G., Pilija, V., 2016. Fatal Intoxication with Toluene Due to Inhalation of Glue. *Journal of Forensic Sciences*, Volume 61, pp. 875–878

Gupta, M.K., Srivastava, R.K., Bisaria, H., 2015. Potential of Jute Fibre Reinforced Polymer Composites : A Review. *International Journal of Fiber and Textile and Research*, Volume 5(3), pp. 30–38

Hörold, A., Schartel, B., Trappe, V., Korzen, M., Bünker, J., 2017. Fire Stability Of Glass-Fibre Sandwich Panels: The Influence of Core Materials And Flame Retardants. *Composite Structures*, Volume 160, pp. 1310–1318

Jeevi, G., Nayak, S.K., Abdul-Kader, M., 2019. Review on Adhesive Joints and Their Application In Hybrid Composite Structures. *Journal of Adhesion Science and Technology*, Volume 33(14), pp. 1497–1520

Kim, N.K., Dutta, S., Bhattacharyya, D., 2018. A review of Flammability of Natural Fibre Reinforced Polymeric Composites. *Composites Science and Technology*, Volume 162, pp. 64–78

Kostin, V., Nasonov, F., Zinin, A., 2021. Influence of Adhesive Bond Line Thickness on Joint Strength of Composite Aircraft Structures. *Journal of Physics: Conference Series*, Volume 1925(1), pp. 724–736.

Ledesma, R., Yost, W., Palmieri, F., Cataldo, D., Connell, J., 2018. Correlation of Optically Stimulated Electron Emission with Failure Mode of Adhesively Bonded Epoxy Composites. *International Journal of Adhesion and Adhesives*, Volume 84, pp. 257–264

Lee, C. H., Salit, M.S., Hassan, M.R., 2014. A Review of The Flammability Factors of Kenaf and Allied Fibre Reinforced Polymer Composites. *Advances in Materials Science and Engineering*, Volume 2014, p. 514036

Liao, B., Yang, L., Ju, X., Peng, Y., Gao, Y., 2020. Experimental Study on Burning and Toxicity Hazards of a PET Laminated Photovoltaic Panel. *Solar Energy Materials and Solar Cells*, Volume 206, p. 110295

Machalická, K., Eliášová, M., 2017. Adhesive Joints in Glass Structures: Effects of Various Materials in The Connection, Thickness of The Adhesive Layer, and Aging. *International Journal of Adhesion and Adhesives*, Volume 72, pp. 10–22

Misnon, M.I., Islam, M.M., Epaarachchi, J.A., Chen, H., Goda, K., Khan, M.T.I., 2018. Flammability Characteristics of Chemical Treated Woven Hemp Fabric Reinforced Vinyl Ester Composites. *Science and Technology of Materials*, Volume 30(3), pp. 174–188

Momber, A.W., Fröck, L., Marquardt, T., 2021. Effects of Adhesive Type on The Mechanical Properties of Adhesive Joints Between Polyurethane Top Coats and Polyurethane-Based Adhesives After Accelerated Atmospheric Aging. *Marine Structures*, Volume 79, p. 103022

Novotný, C., Doubrava, K., Růžička, M., 2017. Testing Of Adhesive Joints In Sandwich Structures. *Materials Today: Proceedings*, Volume 4(5), pp. 5898–5903

Nugroho, P.S., Latief, Y., Wibowo, W., 2022. Structural Equation Modelling For Improving Fire Safety Reliability through Enhancing Fire Safety Management on High-Rise Building. *International Journal of Technology*, Volume 13(4), pp. 740–750

Ogabi, R., Manescau, B., Chetehouna, K., Gascoin, N., 2021. Composites and Their Gaseous Emission Assessment. *Energy*, Volume 14, pp. 1–32

Ortega, R., Monzón, M.D., Ortega, Z.C., Cunningham, E., 2020. Study and Fire Test of Banana Fibre Reinforced Composites with Flame Retardance Properties. *Open Chemistry*, Volume 18(1), pp. 275–286

Parmar, M.S., Singh, M., Tiwari, R.K., Saran, S., 2014. Study on Flame Retardant Properties Of Poly(Lactic Acid) Fiber Fabrics. *Indian Journal of Fibre and Textile Research*, Volume 39(3), pp. 268–273

Pausas, J.G., Keeley, J.E., Schwilk, D.W., 2017. Flammability as an Ecological and Evolutionary Driver. *Journal of Ecology*, Volume 105(2), pp. 289–297

Raajeshkrishna, C.R., Chandramohan, P., 2020. Effect of Reinforcements and Processing Method on Mechanical Properties of Glass and Basalt Epoxy Composites. *SN Applied Sciences*, Volume 2 (5), p. 959

Rupani, S.V., Acharya, G., Jani, S.S., 2017. Design, Modelling and Manufacturing aspects of Honeycomb Sandwich Structures: A Review. *International Journal of Scientific Development and Research*, Volume 2(4), pp. 526–532

Salmeia, K.A., Jovic, M., Ragaisiene, A., Rukuiziene, Z., Milasius, R., Mikucioniene, D., Gaan, S., 2016. Flammability of Cellulose-Based Fibers and The Effect of Structure of Phosphorus Compounds On Their Flame Retardancy. *Polymers*, Volume 8 (8), p. 293

Shang, X., Marques, E.A.S., Carbas, R.J.C., Barbosa, A.Q., Jiang, D., da Silva, L.F.M., Chen, D., Ju, S., 2020. Fracture Mechanism of Adhesive Single-Lap Joints with Composite Adherends Under Quasi-Static Tension. *Composite Structures*, Volume 251, p. 112639

Shavandi, A., Ali, A., 2018. A New Adhesive From Waste Wool Protein Hydrolysate. *Journal of Environmental Chemical Engineering*, Volume 6(5), pp. 6700–6706

Sugiman, Sulardjaka, 2016. Water Absorption and Desorption Behavior and Their Effect on The Tensile Properties of FM 73M Adhesive Film. *International Journal of Technology*, Volume 7(3), pp. 438–446

Suoware, T.O., Ezema, I.C., Edelugo, S.O., 2017. Flammability of Flame Retarded Natural Fibre Composites and Application in Automobile Interior: A Review. *Imperial Journal of Interdisciplinary Research*, Volume 3(8), pp. 2454–1362

Suwondo, R., Cunningham, L., Gillie, M., Suangga, M., Hidayat, I., 2021. Model Parameter Sensitivity for Structural Analysis of Composite Slab Structures in Fire. *International Journal of Technology*, Volume 12(2), pp. 339–348

Szolnoki, B., Bocz, K., Soti, P.L., Bodzay, B., Zimonyi, E., Toldy, A., Morlin, B., Bujnowicz, K., Marosi, G., 2015. Development of Natural Fibre Reinforced Flame Retarded Epoxy Resin Composites. *Polymer Degradation and Stability*, Volume 119, pp. 68–76

Tualeka, A.R., Wibrata, D.A., Ilmi, B., Ahsan, A., Rahmawati, P., 2019. Association Between Toluene Inhalation Exposure and Demography Towards Risk of Neurotoxic: A Cross-Sectional Study at Plastic Sack Industry Workers in Indonesia. *Global Journal of Health Science*, Volume 11(2), p. 20

Valente, J.P.A., Campilho, R.D.S.G., Marques, E.A.S., Machado, J.J.M., Da Silva, L.F.M., 2019. Adhesive Joint Analysis Under Tensile Impact Loads By Cohesive Zone Modelling. *Composite Structures*, Volume 222, p. 110894

Vinod, A., Tengsuthiwat, J., Gowda, Y., Vijay, R., Sanjay, M.R., Siengchin, S., Dhakal, H.N., 2022. Jute/Hemp Bio-Epoxy Hybrid Bio-Composites: Influence of Stacking Sequence on Adhesion of Fiber-Matrix. *International Journal of Adhesion and Adhesives*, Volume 113, p. 103050

Wang, W., Wang, D., Xia, B., Li, T., Wang, Y., Zhang, X., Bai, H.,Chen, M., Dong, W., 2022. Rigid Polyurethane Foams Based on Dextrin and Glycerol. *Industrial Crops and Products*, Volume 177, p. 114479

Wei, X., Xiong, J., Wang, J., Xu, W., 2020. New Advances in Fiber-Reinforced Composite Honeycomb Materials. *Science China Technological Sciences*, Volume 63(8), pp. 1348–1370

Zhu, C., Li, S., Li, J., Clement, M., Rudd, C., Yi, X., Liu, X., 2020. Fie Performance of Sandwich Composites with Intumescent Mat Protection: Evolving Thermal Insulation, Post-Fire Performance and Rail Industry Testing. *Fire Safety Journal*, Volume 116, p. 103205